Measurement of the *WZ* cross section and triple gauge couplings in $p\bar{p}$ collisions at $\sqrt{s} = 1.96$ TeV

T. Aaltonen,[21] B. Álvarez González,[9,aa] S. Amerio,[40a] D. Amidei,[32] A. Anastassov,[15,y] A. Annovi,[17] J. Antos,[12] G. Apollinari,[15] J. A. Appel,[15] T. Arisawa,[54] A. Artikov,[13] J. Asaadi,[49] W. Ashmanskas,[15] B. Auerbach,[57] A. Aurisano,[49] F. Azfar,[39] W. Badgett,[15] T. Bae,[25] A. Barbaro-Galtieri,[26] V. E. Barnes,[44] B. A. Barnett,[23] P. Barria,[42a,42c] P. Bartos,[12] M. Bauce,[40a,40b] F. Bedeschi,[42a] S. Behari,[23] G. Bellettini,[42a,42b] J. Bellinger,[56] D. Benjamin,[14] A. Beretvas,[15] A. Bhatti,[46] D. Bisello,[40a,40b] I. Bizjak,[28] K. R. Bland,[5] B. Blumenfeld,[23] A. Bocci,[14] A. Bodek,[45] D. Bortoletto,[44] J. Boudreau,[43] A. Boveia,[11] L. Brigliadori,[6a,6b] C. Bromberg,[33] E. Brucken,[21] J. Budagov,[13] H. S. Budd,[45] K. Burkett,[15] G. Busetto,[40a,40b] P. Bussey,[19] A. Buzatu,[31] A. Calamba,[10] C. Calancha,[29] S. Camarda,[4] M. Campanelli,[28] M. Campbell,[32] F. Canelli,[11,15] B. Carls,[22] D. Carlsmith,[56] R. Carosi,[42a] S. Carrillo,[16,n] S. Carron,[15] B. Casal,[9,l] M. Casarsa,[50a] A. Castro,[6a,6b] P. Catastini,[20] D. Cauz,[50a] V. Cavaliere,[22] M. Cavalli-Sforza,[4] A. Cerri,[26,g] L. Cerrito,[28,t] Y. C. Chen,[1] M. Chertok,[7] G. Chiarelli,[42a] G. Chlachidze,[15] F. Chlebana,[15] K. Cho,[25] D. Chokheli,[13] W. H. Chung,[56] Y. S. Chung,[45] M. A. Ciocci,[42a,42c] A. Clark,[18] C. Clarke,[55] G. Compostella,[40a,40b] M. E. Convery,[15] J. Conway,[7] M. Corbo,[15] M. Cordelli,[17] C. A. Cox,[7] D. J. Cox,[7] F. Crescioli,[42a,42b] J. Cuevas,[9,aa] R. Culbertson,[15] D. Dagenhart,[15] N. d'Ascenzo,[15,x] M. Datta,[15] P. de Barbaro,[45] M. Dell'Orso,[42a,42b] L. Demortier,[46] M. Deninno,[6a] F. Devoto,[21] M. d'Errico,[40a,40b] A. Di Canto,[42a,42b] B. Di Ruzza,[15] J. R. Dittmann,[5] M. D'Onofrio,[27] S. Donati,[42a,42b] P. Dong,[15] M. Dorigo,[50a] T. Dorigo,[40a] K. Ebina,[54] A. Elagin,[49] A. Eppig,[32] R. Erbacher,[7] S. Errede,[22] N. Ershaidat,[15,ee] R. Eusebi,[49] S. Farrington,[39] M. Feindt,[24] J. P. Fernandez,[29] R. Field,[16] G. Flanagan,[15,v] R. Forrest,[7] M. J. Frank,[5] M. Franklin,[20] J. C. Freeman,[15] Y. Funakoshi,[54] I. Furic,[16] M. Gallinaro,[46] J. E. Garcia,[18] A. F. Garfinkel,[44] P. Garosi,[42a,42c] H. Gerberich,[22] E. Gerchtein,[15] S. Giagu,[47a] V. Giakoumopoulou,[3] P. Giannetti,[42a] K. Gibson,[43] C. M. Ginsburg,[15] N. Giokaris,[3] P. Giromini,[17] G. Giurgiu,[23] V. Glagolev,[13] D. Glenzinski,[15] M. Gold,[35] D. Goldin,[49] N. Goldschmidt,[16] A. Golossanov,[15] G. Gomez,[9] G. Gomez-Ceballos,[30] M. Goncharov,[30] O. González,[29] I. Gorelov,[35] A. T. Goshaw,[14] K. Goulianos,[46] S. Grinstein,[4] C. Grosso-Pilcher,[11] R. C. Group,[53,15] J. Guimaraes da Costa,[20] S. R. Hahn,[15] E. Halkiadakis,[48] A. Hamaguchi,[38] J. Y. Han,[45] F. Happacher,[17] K. Hara,[51] D. Hare,[48] M. Hare,[52] R. F. Harr,[55] K. Hatakeyama,[5] C. Hays,[39] M. Heck,[24] J. Heinrich,[41] M. Herndon,[56] S. Hewamanage,[5] D. Hidas,[48] A. Hocker,[15] W. Hopkins,[15,h] D. Horn,[24] S. Hou,[1] R. E. Hughes,[36] M. Hurwitz,[11] U. Husemann,[57] N. Hussain,[31] M. Hussein,[33] J. Huston,[33] G. Introzzi,[42a] M. Iori,[47a,47b] A. Ivanov,[7,q] E. James,[15] D. Jang,[10] B. Jayatilaka,[14] E. J. Jeon,[25] S. Jindariani,[15] M. Jones,[44] K. K. Joo,[25] S. Y. Jun,[10] T. R. Junk,[15] T. Kamon,[25,49] P. E. Karchin,[55] A. Kasmi,[5] Y. Kato,[38,p] W. Ketchum,[11] J. Keung,[41] V. Khotilovich,[49] B. Kilminster,[15] D. H. Kim,[25] H. S. Kim,[25] J. E. Kim,[25] M. J. Kim,[17] S. B. Kim,[25] S. H. Kim,[51] Y. K. Kim,[11] Y. J. Kim,[25] N. Kimura,[54] M. Kirby,[15] S. Klimenko,[16] K. Knoepfel,[15] K. Kondo,[54,a] D. J. Kong,[25] J. Konigsberg,[16] A. V. Kotwal,[14] M. Kreps,[24] J. Kroll,[41] D. Krop,[11] M. Kruse,[14] V. Krutelyov,[49,d] T. Kuhr,[24] M. Kurata,[51] S. Kwang,[11] A. T. Laasanen,[44] S. Lami,[42a] S. Lammel,[15] M. Lancaster,[28] R. L. Lander,[7] K. Lannon,[36,z] A. Lath,[48] G. Latino,[42a,42c] T. LeCompte,[2] E. Lee,[49] H. S. Lee,[11,r] J. S. Lee,[25] S. W. Lee,[49,cc] S. Leo,[42a,42b] S. Leone,[42a] J. D. Lewis,[15] A. Limosani,[14,u] C.-J. Lin,[26] M. Lindgren,[15] E. Lipeles,[41] A. Lister,[18] D. O. Litvintsev,[15] C. Liu,[43] H. Liu,[53] Q. Liu,[44] T. Liu,[15] S. Lockwitz,[57] A. Loginov,[57] D. Lucchesi,[40a,40b] J. Lueck,[24] P. Lujan,[26] P. Lukens,[15] G. Lungu,[46] J. Lys,[26] R. Lysak,[12,f] R. Madrak,[15] K. Maeshima,[15] P. Maestro,[42a,42c] S. Malik,[46] G. Manca,[27,b] A. Manousakis-Katsikakis,[3] F. Margaroli,[47a] C. Marino,[24] M. Martínez,[4] P. Mastrandrea,[47a] K. Matera,[22] M. E. Mattson,[55] A. Mazzacane,[15] P. Mazzanti,[6a] K. S. McFarland,[45] P. McIntyre,[49] R. McNulty,[27,k] A. Mehta,[27] P. Mehtala,[21] C. Mesropian,[46] T. Miao,[15] D. Mietlicki,[32] A. Mitra,[1] H. Miyake,[51] S. Moed,[15] N. Moggi,[6a] M. N. Mondragon,[15,n] C. S. Moon,[25] R. Moore,[15] M. J. Morello,[42a,42d] J. Morlock,[24] P. Movilla Fernandez,[15] A. Mukherjee,[15] Th. Muller,[24] P. Murat,[15] M. Mussini,[6a,6b] J. Nachtman,[15,o] Y. Nagai,[51] J. Naganoma,[54] I. Nakano,[37] A. Napier,[52] J. Nett,[49] C. Neu,[53] M. S. Neubauer,[22] J. Nielsen,[26,e] L. Nodulman,[2] S. Y. Noh,[25] O. Norniella,[22] L. Oakes,[39] S. H. Oh,[14] Y. D. Oh,[25] I. Oksuzian,[53] T. Okusawa,[38] R. Orava,[21] L. Ortolan,[4] S. Pagan Griso,[40a,40b] C. Pagliarone,[50a] E. Palencia,[9,g] V. Papadimitriou,[15] A. A. Paramonov,[2] J. Patrick,[15] G. Pauletta,[50a,50b] M. Paulini,[10] C. Paus,[30] D. E. Pellett,[7] A. Penzo,[50a] T. J. Phillips,[14] G. Piacentino,[42a] E. Pianori,[41] J. Pilot,[36] K. Pitts,[22] C. Plager,[8] L. Pondrom,[56] S. Poprocki,[15,h] K. Potamianos,[44] F. Prokoshin,[13,dd] A. Pranko,[26] F. Ptohos,[17,i] G. Punzi,[42a,42b] J. Pursley,[56] A. Rahaman,[43] V. Ramakrishnan,[56] N. Ranjan,[44] I. Redondo,[29] P. Renton,[39] M. Rescigno,[47a] T. Riddick,[28] F. Rimondi,[6a,6b] L. Ristori,[42a,15] A. Robson,[19] T. Rodrigo,[9] T. Rodriguez,[41] E. Rogers,[22] S. Rolli,[52,j] R. Roser,[15] F. Ruffini,[42a,42c] A. Ruiz,[9] J. Russ,[10] V. Rusu,[15] A. Safonov,[49] W. K. Sakumoto,[45] Y. Sakurai,[54] L. Santi,[50a,50b] K. Sato,[51] V. Saveliev,[15,x] A. Savoy-Navarro,[15,bb] P. Schlabach,[15] A. Schmidt,[24] E. E. Schmidt,[15] T. Schwarz,[15] L. Scodellaro,[9] A. Scribano,[42a,42c] F. Scuri,[42a] S. Seidel,[35] Y. Seiya,[38] A. Semenov,[13] F. Sforza,[42a,42c] S. Z. Shalhout,[7] T. Shears,[27] P. F. Shepard,[43] M. Shimojima,[51,w] M. Shochet,[11] I. Shreyber-Tecker,[34] A. Simonenko,[13] P. Sinervo,[31] K. Sliwa,[52] J. R. Smith,[7] F. D. Snider,[15] A. Soha,[15] V. Sorin,[4] H. Song,[43]

P. Squillacioti,[42a,42c] M. Stancari,[15] R. St. Denis,[19] B. Stelzer,[31] O. Stelzer-Chilton,[31] D. Stentz,[15,y] J. Strologas,[35] G. L. Strycker,[32] Y. Sudo,[51] A. Sukhanov,[15] I. Suslov,[13] K. Takemasa,[51] Y. Takeuchi,[51] J. Tang,[11] M. Tecchio,[32] P. K. Teng,[1] J. Thom,[15,h] J. Thome,[10] G. A. Thompson,[22] E. Thomson,[41] D. Toback,[49] S. Tokar,[12] K. Tollefson,[33] T. Tomura,[51] D. Tonelli,[15] S. Torre,[17] D. Torretta,[15] P. Totaro,[40a] M. Trovato,[42a,42d] F. Ukegawa,[51] S. Uozumi,[25] R. Vanguri,[41] A. Varganov,[32] F. Vázquez,[16,n] G. Velev,[15] C. Vellidis,[15] M. Vidal,[44] I. Vila,[9] R. Vilar,[9] J. Vizán,[9] M. Vogel,[35] G. Volpi,[17] P. Wagner,[41] R. L. Wagner,[15] T. Wakisaka,[38] R. Wallny,[8] S. M. Wang,[1] A. Warburton,[31] D. Waters,[28] W. C. Wester III,[15] D. Whiteson,[41,c] A. B. Wicklund,[2] E. Wicklund,[15] S. Wilbur,[11] F. Wick,[24] H. H. Williams,[41] J. S. Wilson,[36] P. Wilson,[15] B. L. Winer,[36] P. Wittich,[15,h] S. Wolbers,[15] H. Wolfe,[36] T. Wright,[32] X. Wu,[18] Z. Wu,[5] K. Yamamoto,[38] D. Yamato,[38] T. Yang,[15] U. K. Yang,[11,s] Y. C. Yang,[25] W.-M. Yao,[26] G. P. Yeh,[15] K. Yi,[15,o] J. Yoh,[15] K. Yorita,[54] T. Yoshida,[38,m] G. B. Yu,[14] I. Yu,[25] S. S. Yu,[15] J. C. Yun,[15] A. Zanetti,[50a] Y. Zeng,[14] C. Zhou,[14] and S. Zucchelli[6a,6b]

(CDF Collaboration)

[1]*Institute of Physics, Academia Sinica, Taipei, Taiwan 11529, Republic of China*
[2]*Argonne National Laboratory, Argonne, Illinois 60439, USA*
[3]*University of Athens, 157 71 Athens, Greece*
[4]*Institut de Fisica d'Altes Energies, ICREA, Universitat Autonoma de Barcelona, E-08193, Bellaterra (Barcelona), Spain*
[5]*Baylor University, Waco, Texas 76798, USA*
[6a]*Istituto Nazionale di Fisica Nucleare Bologna, I-40127 Bologna, Italy*
[6b]*University of Bologna, I-40127 Bologna, Italy*
[7]*University of California, Davis, Davis, California 95616, USA*
[8]*University of California, Los Angeles, Los Angeles, California 90024, USA*
[9]*Instituto de Fisica de Cantabria, CSIC-University of Cantabria, 39005 Santander, Spain*
[10]*Carnegie Mellon University, Pittsburgh, Pennsylvania 15213, USA*
[11]*Enrico Fermi Institute, University of Chicago, Chicago, Illinois 60637, USA*
[12]*Comenius University, 842 48 Bratislava, Slovakia; Institute of Experimental Physics, 040 01 Kosice, Slovakia*
[13]*Joint Institute for Nuclear Research, RU-141980 Dubna, Russia*
[14]*Duke University, Durham, North Carolina 27708, USA*
[15]*Fermi National Accelerator Laboratory, Batavia, Illinois 60510, USA*
[16]*University of Florida, Gainesville, Florida 32611, USA*
[17]*Laboratori Nazionali di Frascati, Istituto Nazionale di Fisica Nucleare, I-00044 Frascati, Italy*
[18]*University of Geneva, CH-1211 Geneva 4, Switzerland*
[19]*Glasgow University, Glasgow G12 8QQ, United Kingdom*
[20]*Harvard University, Cambridge, Massachusetts 02138, USA*
[21]*Division of High Energy Physics, Department of Physics, University of Helsinki and Helsinki Institute of Physics,*
FIN-00014, Helsinki, Finland
[22]*University of Illinois, Urbana, Illinois 61801, USA*
[23]*The Johns Hopkins University, Baltimore, Maryland 21218, USA*
[24]*Institut für Experimentelle Kernphysik, Karlsruhe Institute of Technology, D-76131 Karlsruhe, Germany*
[25]*Center for High Energy Physics: Kyungpook National University, Daegu 702-701, Korea;*
Seoul National University, Seoul 151-742, Korea;
Sungkyunkwan University, Suwon 440-746, Korea;
Korea Institute of Science and Technology Information, Daejeon 305-806, Korea;
Chonnam National University, Gwangju 500-757, Korea;
Chonbuk National University, Jeonju 561-756, Korea
[26]*Ernest Orlando Lawrence Berkeley National Laboratory, Berkeley, California 94720, USA*
[27]*University of Liverpool, Liverpool L69 7ZE, United Kingdom*
[28]*University College London, London WC1E 6BT, United Kingdom*
[29]*Centro de Investigaciones Energeticas Medioambientales y Tecnologicas, E-28040 Madrid, Spain*
[30]*Massachusetts Institute of Technology, Cambridge, Massachusetts 02139, USA*
[31]*Institute of Particle Physics: McGill University, Montréal, Québec, Canada H3A 2T8;*
Simon Fraser University, Burnaby, British Columbia, Canada V5A 1S6;
University of Toronto, Toronto, Ontario, Canada M5S 1A7;
and TRIUMF, Vancouver, British Columbia, Canada V6T 2A3
[32]*University of Michigan, Ann Arbor, Michigan 48109, USA*
[33]*Michigan State University, East Lansing, Michigan 48824, USA*
[34]*Institution for Theoretical and Experimental Physics, ITEP, Moscow 117259, Russia*
[35]*University of New Mexico, Albuquerque, New Mexico 87131, USA*

[36]The Ohio State University, Columbus, Ohio 43210, USA
[37]Okayama University, Okayama 700-8530, Japan
[38]Osaka City University, Osaka 588, Japan
[39]University of Oxford, Oxford OX1 3RH, United Kingdom
[40a]Istituto Nazionale di Fisica Nucleare, Sezione di Padova-Trento, I-35131 Padova, Italy
[40b]University of Padova, I-35131 Padova, Italy
[41]University of Pennsylvania, Philadelphia, Pennsylvania 19104, USA
[42a]Istituto Nazionale di Fisica Nucleare Pisa, I-56127 Pisa, Italy
[42b]University of Pisa, I-56127 Pisa, Italy
[42c]University of Siena, I-56127 Pisa, Italy
[42d]Scuola Normale Superiore, I-56127 Pisa, Italy
[43]University of Pittsburgh, Pittsburgh, Pennsylvania 15260, USA
[44]Purdue University, West Lafayette, Indiana 47907, USA
[45]University of Rochester, Rochester, New York 14627, USA
[46]The Rockefeller University, New York, New York 10065, USA
[47a]Istituto Nazionale di Fisica Nucleare, Sezione di Roma 1,
[47b]Sapienza Università di Roma, I-00185 Roma, Italy
[48]Rutgers University, Piscataway, New Jersey 08855, USA
[49]Texas A&M University, College Station, Texas 77843, USA
[50a]Istituto Nazionale di Fisica Nucleare Trieste/Udine, I-34100 Trieste, I-33100 Udine, Italy
[50b]University of Udine, I-33100 Udine, Italy
[51]University of Tsukuba, Tsukuba, Ibaraki 305, Japan
[52]Tufts University, Medford, Massachusetts 02155, USA
[53]University of Virginia, Charlottesville, Virginia 22906, USA
[54]Waseda University, Tokyo 169, Japan
[55]Wayne State University, Detroit, Michigan 48201, USA
[56]University of Wisconsin, Madison, Wisconsin 53706, USA
[57]Yale University, New Haven, Connecticut 06520, USA

[a]Deceased
[b]With visitor from Istituto Nazionale di Fisica Nucleare, Sezione di Cagliari, 09042 Monserrato (Cagliari), Italy
[c]With visitor from University of California Irvine, Irvine, CA 92697, USA
[d]With visitor from University of California Santa Barbara, Santa Barbara, CA 93106, USA
[e]With visitor from University of California Santa Cruz, Santa Cruz, CA 95064, USA
[f]With visitor from Institute of Physics, Academy of Sciences of the Czech Republic, Czech Republic
[g]With visitor from CERN, CH-1211 Geneva, Switzerland
[h]With visitor from Cornell University, Ithaca, NY 14853, USA
[i]With visitor from University of Cyprus, Nicosia CY-1678, Cyprus
[j]With visitor from Office of Science, U.S. Department of Energy, Washington, DC 20585, USA
[k]With visitor from University College Dublin, Dublin 4, Ireland
[l]With visitor from ETH, 8092 Zurich, Switzerland
[m]With visitor from University of Fukui, Fukui City, Fukui Prefecture, Japan 910-0017
[n]With visitor from Universidad Iberoamericana, Mexico D.F., Mex- ico
[o]With visitor from University of Iowa, IA City, IA 52242, USA
[p]With visitor from Kinki University, Higashi-Osaka City, Japan 577-8502
[q]With visitor from Kansas State University, Manhattan, KS 66506, USA
[r]With visitor from Ewha Womans University, Seoul, 120-750, Korea
[s]With visitor from University of Manchester, Manchester M13 9PL, United Kingdom
[t]With visitor from Queen Mary, University of London, London, E1 4NS, United Kingdom
[u]With visitor from University of Melbourne, Victoria 3010, Australia
[v]With visitor from Muons, Inc., Batavia, IL 60510, USA
[w]With visitor from Nagasaki Institute of Applied Science, Nagasaki, Japan
[x]With visitor from National Research Nuclear University, Moscow, Russia
[y]With visitor from Northwestern University, Evanston, IL 60208, USA
[z]With visitor from University of Notre Dame, Notre Dame, IN 46556, USA
[aa]With visitor from Universidad de Oviedo, E-33007 Oviedo, Spain
[bb]With visitor from CNRS-IN2P3, Paris, F-75205 France
[cc]With visitor from Texas Tech University, Lubbock, TX 79609, USA
[dd]With visitor from Universidad Tecnica Federico Santa Maria, 110v Valparaiso, Chile
[ee]With visitor from Yarmouk University, Irbid 211-63, Jordan

This article describes the current most precise measurement of the *WZ* production cross section as well as limits on anomalous *WWZ* couplings at a center-of-mass energy of 1.96 TeV in proton-antiproton collisions for the Collider Detector at Fermilab (CDF). *WZ* candidates are reconstructed from decays containing three charged leptons and missing energy from a neutrino, where the charged leptons are either electrons or muons. Using data collected by the CDF II detector (7.1 fb^{-1} of integrated luminosity), 63 candidate events are observed with the expected background contributing 8 ± 1 events. The measured total cross section $\sigma(p\bar{p} \rightarrow WZ) = 3.93^{+0.60}_{-0.53}(\text{stat})^{+0.59}_{-0.46}(\text{syst})$ pb is in good agreement with the standard model prediction of 3.50 ± 0.21. The same sample is used to set limits on anomalous *WWZ* couplings.

The measurement of *WZ* production is an important test of the standard model (SM) of particle physics. *WZ* pairs are produced both in *s*-channel ($q\bar{q} \rightarrow W^* \rightarrow WZ$) and in *t*-channel ($q\bar{q} \rightarrow WZ$) interactions. The *WZ* production is unique in that the *s*-channel mode of production provides sensitivity to the *WWZ* vertex, which is governed by triple-gauge boson couplings (TGCs); the presence of anomalous couplings [1] could be an indication of new physics at a higher mass scale leading to different rates and kinematic distributions than predicted by the SM. Furthermore, this process is an essential background for Higgs boson searches at particle colliders because the *WZ* decay into leptons is the primary background to high mass Higgs boson searches in the three-lepton signature, as well as an important background process in two-lepton Higgs boson analyses [2].

This article reports a measurement of the *WZ* production cross section and limits on anomalous TGCs using a final state consisting of three charged leptons and one neutrino in $p\bar{p}$ collision data collected by the CDF II detector from 7.1 fb^{-1} of integrated luminosity. The $WZ \rightarrow l\nu ll$ decay, where *l* is an electron or muon and ν is a neutrino contributing missing energy, allows for the reconstruction of a variety of kinematic quantities that are utilized to distinguish signal from background by training a neural network [3]. The cross section is then extracted from the output of the neural network by fitting the shape with a maximum likelihood method. Limits on anomalous TGCs are set by analyzing the shape of the component of the momentum of the *Z* boson that is transverse to the beam line as a discriminant.

The $SU(2)_L \times U(1)_Y$ part of the SM implies that *W* and *Z* weak vector bosons may interact via trilinear or quartic vertices. The *WZ* cross section is proportional to the interaction coupling strength predicted by the SM as $e \cot\theta_W$, where *e* is the electric charge and θ_W is the weak mixing angle. We want to measure the cross section of the process $p\bar{p} \rightarrow WZ$, whose expected value in the limit of zero *W* and *Z* boson decay widths is 3.50 pb [4,5]. We therefore measure the cross section by performing a likelihood fit to a parameter representing the ratio of the measured to expected *WZ* cross section, to be discussed below.

The cross section of this process was first reported by CDF with 1.1 fb^{-1} [6] in 2007. Subsequently, D0 reported

with 1.0 fb^{-1} [7] in 2005, updated with 4.1 fb^{-1} [8] in 2007, and again with 8.6 fb^{-1} [9] in 2012. Limits on anomalous TGCs were reported previously by LEP2 [10], by D0 [11], and recently by CMS [12] and ATLAS [13]. All results reported measurements consistent with the standard model. This analysis describes CDF's most precise measurement of the *WZ* cross section and TGCs.

In the CDF II detector [14], a particle's direction is characterized by the azimuthal angle ϕ and the pseudorapidity $\eta = -\ln[\tan(\theta/2)]$, where θ is the polar angle measured with respect to the proton beam direction. The transverse energy E_T is defined as $E \sin\theta$, where *E* is the energy in the electromagnetic and hadronic calorimeter towers associated with a cluster of energy deposition. The transverse momentum p_T is the particle's momentum component transverse to the beam line. The magnitude of the p_T for an electron is scaled according to the energy measured in the calorimeter in order to account for momentum loss from final state radiation and bremsstrahlung. The missing transverse energy vector $\vec{\not{E}}_T$ is defined as $-\sum_i E_T^i \hat{n}_T^i$, where the index *i* loops over all towers of the calorimeter and $\hat{n}_T^i$ is the unit vector in the transverse plane pointing from the interaction point to the energy deposition in calorimeter tower *i*. The $\vec{\not{E}}_T$ is corrected for the p_T of muons, which do not deposit all of their energy in the calorimeter, and tracks that point to uninstrumented regions in the calorimeter. The scalar missing transverse energy is defined as $|\vec{\not{E}}_T|$ and denoted as $\not{E}_T$. Strongly interacting partons produced in the $p\bar{p}$ collision undergo fragmentation that results in highly collimated jets of hadronic particles. Jet candidates are reconstructed using the calorimeter signals and are required to have $E_T > 15$ GeV and $|\eta| < 2.5$. Isolated lepton candidates are accepted out to an $|\eta|$ of 2.0 for electron candidates and $|\eta|$ of 1.0 for muon candidates.

The experimental signature for the decay $WZ \rightarrow l\nu ll$ is reconstructed as three charged leptons (electrons or muons) and $\not{E}_T$ from the neutrino(s) that escaped undetected. Events are also detected if the *W* or *Z* decays to tau lepton(s) and those tau(s) subsequently decay to detectable electrons or muons—these events are considered part of the signal. Consequently, events containing three charged leptons, not all with the same charge, are selected from the data sample. The online event triggering and selection of

lepton candidates are identical to those used in the search for SM Higgs bosons decaying to two *W* bosons at CDF [2]. Our baseline event selection is to require the leading lepton's E_T (or p_T for muons) to be above 20 GeV (GeV/c) to satisfy the trigger requirements, while the second and third leptons are allowed to have an E_T (p_T) as low as 10 GeV (GeV/c). Additionally, because the neutrino in the $W \rightarrow l\nu$ decay carries undetected energy, the $WZ \rightarrow l\nu ll$ process tends to produce events with higher missing energy than the background processes—aside from $t\bar{t}$ whose $\not{E}_T$ distribution is also similarly high valued but is a nearly negligible background. We therefore require $\not{E}_T > 25$ GeV.

Lastly, the dominant background remaining after these cuts is SM *ZZ* production. This motivates two more cuts to require one and only one $Z \rightarrow ll$ candidate in the event. We make a standard *Z* boson identification cut by requiring events to have a pair of same-flavor, opposite-signed leptons whose two-lepton mass falls within a window of ± 15 GeV/c^2 around the *Z* mass. This removes most of the SM backgrounds with no *Z* in the final state. We note that this cut reduces $Z\gamma \rightarrow ll\gamma$ events because the dilepton mass would not reconstruct back to the *Z* when the γ is emitted by one of the two leptons. In that case, the two-lepton mass underestimates the *Z* mass because the three-body ($ll\gamma$) mass is what reconstructs the *Z*.

To further reduce the $ZZ \rightarrow llll$ background, we reject any event with an extra track with $p_T > 8$ GeV/c, thereby rejecting events that may have a fourth lepton that failed to be identified. This cut reduces the remaining *ZZ* background by $\sim 36\%$ while leaving the *WZ* signal contribution essentially unchanged. Even so, *ZZ* remains the primary background in this measurement.

There are several SM processes that result in a similar final state to *WZ* and are backgrounds in this measurement. The aforementioned $ZZ \rightarrow llll$ process appears as a background when one of the four leptons fails to be reconstructed by the detector. This leaves three reconstructed leptons with the one lepton failing reconstruction providing the missing energy signature. Drell–Yan events produced in association with hadronic jets that mimic the signature of a third lepton as well as Drell–Yan pairs produced with an associated photon that converts to an electron-positron pair via interaction with the detector are also significant backgrounds. Lastly, top quark pair production ($t\bar{t} \rightarrow W^+ b W^- \bar{b}$) provides a minor contribution to the background when one of the subsequent *b*-quark jets mimics a lepton signature. The sum of these four backgrounds is quite small compared to the expected signal in the signal kinematics region.

The background modeling—with the exception of the $Z + \text{jets}$ background—is Monte Carlo simulated. Events from *WZ*, *ZZ*, and $t\bar{t}$ are simulated using the PYTHIA [15] generator. The $Z\gamma$ background is determined using the generator described in Ref. [16]. The response of the

TABLE I. Expected number of signal (*WZ*) and background events along with the total number of expected and observed events in the data. Uncertainties include all systematic uncertainties described in the text.

Process	Events		
ZZ	3.6	±	0.5
Z + jets	3.4	±	0.8
Zγ	0.8	±	0.3
$t\bar{t}$	0.1	±	0.04
Total background	7.9	±	1.0
WZ	47.4	±	4.8
Total expected	55.3	±	4.9
Data	63		

CDF II detector is modeled with a GEANT3-based simulation [17] program. The expected yields for each process are normalized to the cross sections calculated at partial next-to-next-to-leading order ($t\bar{t}$ [18]), next-to-leading order (*WZ* and *ZZ* [4]), or leading order with an estimated normalization correction to account for higher orders ($Z\gamma$ [16]). Efficiency corrections for the simulated detector response to lepton candidates are determined using samples of observed $Z \rightarrow l^+l^-$ events. The $Z + \text{jets}$ background normalization is calculated using the probability that a hadronic jet will be reconstructed as a lepton candidate (the same as is done in CDF's $H \rightarrow WW$ search [2]), which is measured in independent jet-triggered data samples. These probabilities are applied to the jets in the $Z + \text{jets}$ data sample to estimate the number of such events that will pass the lepton identification and signal selection criteria. The expected signal and background contributions are given in Table I along with the observed number of events.

The dominant systematic uncertainties on the estimated contributions come from the luminosity measurement (6%) [19] and the simulated acceptances of the signal and background processes. The acceptance uncertainty due to the parton distribution function modeling ranges from 2.1% to 2.7% for the various processes. A 10% uncertainty is assigned to *WZ* and *ZZ* processes for the kinematic differences between leading-order and higher-order calculations. The cross section uncertainty is 6% on the *ZZ* process, 7% on $t\bar{t}$, and 5% on $Z\gamma$. The $Z\gamma$ process has another 20% uncertainty that accounts for possible mismodeling of the rate at which the γ is misidentified as a lepton. Similarly, there is a 25% (23%) uncertainty for $Z + \text{jets}$ ($t\bar{t}$) for mismodeling the rate at which light jets (*b* jets) are misidentified as a lepton. The uncertainty for the modeling of lepton identification is 2% and of trigger efficiencies is 5.4%. Lastly, uncertainties for overall rates for the modeling of jets accounts for 1.2%.

Within the signal kinematic region, we seek to further isolate the signal from background by utilizing a NeuroBayes neural network treatment [3]. In general, the benefits of using a neural network (NN) over a simple

counting experiment are twofold: it can better isolate the signal from the background and provide a single distribution from which the cross section value can be extracted by fitting the data to the shape of the expected physical processes. We train a neural network with a combination of background events and simulated signal events. The input variables for the NN are kinematic quantities selected to exploit differences between signal and background distributions. Starting with many quantities that show relatively small differences in the distributions of backgrounds and signal, a neural network will assign a numerical score whose distribution for backgrounds and signal will be better separated than in any single input quantity alone. The $\not{E}_T$ is a very useful input quantity for the NN because the $W \to l\nu$ decay in the signal yields a $\not{E}_T$ distribution with higher values than the backgrounds. Similarly, the azimuthal angle distribution between the W lepton and the $\not{E}_T$ is useful for distinguishing WZ from the backgrounds because they do not contain W decays. The total energy transverse to the beam line deposited by the WZ decay compared to that of background processes and lepton flavor combinations (eee, $ee\mu$, $e\mu$ track, etc.) are also examples of NN input variables used. Figure 1 shows the output of the NN treatment, with backgroundlike events in simulation and data trending toward a value of -1 while signal-like events trend toward $+1$. Note that $t\bar{t}$ is represented in Fig. 1, but has too small of a contribution to be visible.

The measured cross section for WZ is extracted from the NN output in Fig. 1 with a binned maximum likelihood fit method. The likelihood function is formed from a product of Poisson probabilities for each bin in the NN output, and Gaussian constraints are applied corresponding to each systematic uncertainty:

$$\mathcal{L} = \left(\prod_i \frac{\mu_i^{n_i} e^{-\mu_i}}{n_i!} \right) \cdot \prod_c e^{(-S_c^2/2)}, \qquad (1)$$

where μ_i is the total expectation in the ith bin, n_i is the number of data events in the ith bin, and S_c is a floating parameter associated with the systematic uncertainty c. The μ_i parameter is given by

$$\mu_i = \sum_k \left(\frac{\sigma^{\text{measured}}}{\sigma^{\text{expected}}} \right)_k \left[\prod_c (1 + f_k^c S_c) \right] (N_k^{\text{expected}})_i. \qquad (2)$$

The sum k is over the five processes (one signal and four background) that can contribute to events in bin i, and f_k^c is the fractional uncertainty for the process k due to the systematic uncertainty c. Some systematic uncertainties are common to more than one process and so are correlated. These correlations are accounted for in the definition of μ_i through the f_k^c parameters. The $(N_k^{\text{expected}})_i$ is the expected number of events from process k in the ith bin. All the background processes are constrained to their SM expectations by setting the proportion of measured to expected cross section to unity. The likelihood is then maximized with respect to the floating systematic (S_c) and cross section proportion $(\frac{\sigma^{\text{measured}}}{\sigma^{\text{expected}}})_{WZ}$ parameters, where σ^{expected} is the expected signal cross section and σ^{measured} is the WZ cross section ultimately measured from the data. This method gives a measured value for the WZ cross section of $\sigma(p\bar{p} \to WZ) = 3.93^{+0.60}_{-0.53}(\text{stat})^{+0.59}_{-0.46}(\text{syst})$ pb, which is in good agreement with the aforementioned standard model prediction of 3.50 ± 0.21 [4,5].

The shape and normalization of the p_T spectrum of the Z boson (Fig. 2) are used to place limits on anomalous TGCs. The most general modification of the WWZ vertex preserving C and P separately is parametrized by λ_Z, g_1^Z, and κ_Z [20]. In the SM, $\lambda_Z = \Delta g_1^Z = \Delta \kappa_Z = 0$ where Δg_1^Z and
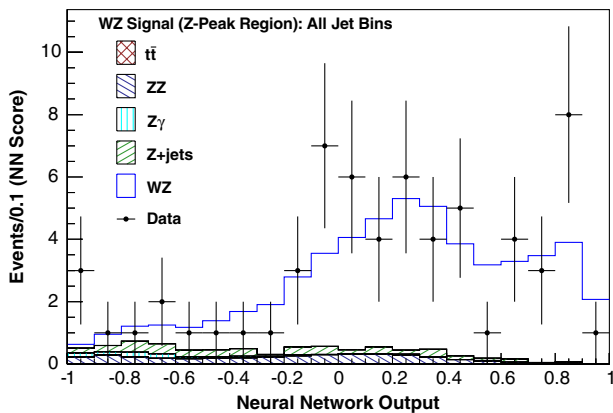

FIG. 1 (color online). The NN output for discriminating the WZ signal events from background processes within the selected signal sample. Note that the $t\bar{t}$ contribution is small enough to not be visible. The processes are stacked.
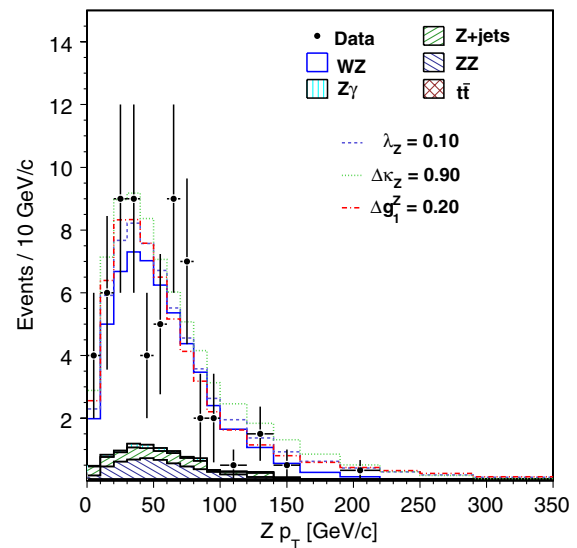

FIG. 2 (color online). The Z p_T distributions for data compared to the SM expectation for signal (WZ) and background. Also presented is how the signal expectation would change with the introduction of anomalous couplings near the observed limits. The processes are stacked.

TABLE II. Expected and observed limits on anomalous TGCs. For each coupling limit set, the two other couplings are constrained at their SM values. Values of the couplings outside the given observed range are excluded at the 95% confidence level.

	Λ (TeV)	λ_Z	Δg_1^Z	$\Delta\kappa_Z$
Exp.	1.5	$(-0.11, 0.12)$	$(-0.12, 0.23)$	$(-0.58, 0.94)$
Obs.	1.5	$(-0.09, 0.11)$	$(-0.09, 0.22)$	$(-0.42, 0.99)$
Exp.	2.0	$(-0.10, 0.10)$	$(-0.11, 0.20)$	$(-0.53, 0.86)$
Obs.	2.0	$(-0.08, 0.10)$	$(-0.08, 0.20)$	$(-0.39, 0.90)$

$\Delta\kappa_Z$ are used to denote the deviations of g_1^Z and κ_Z from their SM values. In general, the parameters λ_z, Δg_1^Z, and $\Delta\kappa_Z$ can be functions of the invariant mass $\sqrt{\hat{s}}$ of the *WZ* system. Nonzero values of λ_Z, g_1^Z, and κ_Z at large $\hat{s}$ violate unitarity. To avoid this, each coupling is modified by a form factor $\alpha(\hat{s}) = \frac{\alpha_0}{(1+\hat{s}/\Lambda^2)^2}$, where α_0 is the unmodified coupling λ_z, g_1^Z, or κ_Z.

The likelihood of the Z p_T distribution for various anomalous TGC models is used to set limits. The expected Z p_T distribution for a given TGC before the effect of the detector response is obtained using MCFM [4]. The detector acceptance and efficiency are modeled by multiplying the MCFM distribution by a Z p_T-dependent factor. This factor is calculated using six different simulated event samples generated at different TGC values with the full detector response simulated by GEANT3. The TGC values are chosen to be in the parameter space near the existing limits. For each sample, the product of acceptance and efficiency is extracted from the simulation as a ratio of the reconstructed and generated yields. These ratios are averaged together as a function of Z p_T using the maximum variation as an estimate of the uncertainty due to assuming the efficiency and acceptance are not dependent on the TGC values.

A likelihood for each of the couplings, $\mathcal{L}(\lambda_Z)$, $\mathcal{L}(\Delta g_1^Z)$, and $\mathcal{L}(\Delta\kappa_Z)$, is computed as a product of the Poisson probability of each of the bins of the Z p_T distribution for the assumed anomalous coupling. Then 95% confidence levels are set where $(-2\ln\mathcal{L}) - (-2\ln\mathcal{L}_{\min}) = (1.96)^2$. The systematic uncertainties include everything considered for the *WZ* cross section and the additional p_T-dependent uncertainty on the efficiency, which ranges from 5% to 20%. Systematic uncertainties are implemented in a way that most reduces the TGC limit sensitivity when fluctuating the signal and background by 1 standard deviation, thereby taking a conservative approach in assigning systematic uncertainty. The observed 95% confidence level limits are consistent with expectations as shown in Table II.

To summarize, the *WZ* production cross section has been measured in $p\bar{p}$ collisions at $\sqrt{s} = 1.96$ TeV from reconstructed events in the trilepton plus $\not{E}_T$ final state using a likelihood ratio formed from a NeuroBayes neural network distribution that discriminates signal from background. This result, $\sigma(p\bar{p} \to WZ) = 3.93^{+0.60}_{-0.53}(\text{stat})^{+0.59}_{-0.46}(\text{syst})$ pb, is the most precise measurement at this energy with an overall uncertainty of less than 20% and in agreement with SM predictions. The same event sample is also used to perform the most sensitive probe to date at this energy of anomalous *WWZ* couplings. The Z p_T distribution of the sample is found to be in agreement with the SM expectation and is used to place limits on anomalous triple-gauge couplings.

[1] J. Ellison and J. Wudka, Annu. Rev. Nucl. Part. Sci. **48**, 33 (1998).
[2] T. Aaltonen *et al.* (CDF Collaboration), Phys. Rev. Lett. **102**, 021802 (2009).
[3] M. Feindt and U. Kerzel, Nucl. Instrum. Methods Phys. Res., Sect. A **559**, 190 (2006).
[4] J. M. Campbell and R. K. Ellis, Phys. Rev. D **60**, 113006 (1999).
[5] A. D. Martin, W. J. Stirling, R. S. Thorne, and G. Watt, Eur. Phys. J. C **63**, 189 (2009).
[6] M. Neubauer *et al.*, Phys. Rev. Lett. **98**, 161801 (2007).
[7] V. M. Abazov *et al.*, Phys. Rev. D **76**, 111104 (2007).
[8] V. M. Abazov *et al.*, Phys. Rev. Lett. **104**, 061801 (2010).
[9] V. M. Abazov *et al.* (D0 Collaboration), Phys. Rev. D **85**, 112005 (2012).

[10] LEP2 Collaboration, *Proceedings of the 10th Lomonosov Conference on Elementary Particle Physics, Moscow, 2001* (World Scientific, Singapore, 2003).

[11] V. M. Abazov *et al.* (D0 Collaboration), Phys. Lett. B **695**, 67 (2011).

[12] CMS Collaboration, EPJ Web Conf. **28**, 06002 (2012).

[13] ATLAS Collaboration, Phys. Rev. B **709**, 341 (2012).

[14] A. Abulencia *et al.* (CDF Collaboration), J. Phys. G **34**, 2457 (2007).

[15] T. Sjostrand, S. Mrenna, and P. Skands, J. High Energy Phys. 05 (2006) 026.

[16] U. Baur, T. Han, and J. Ohnemus, Phys. Rev. D **57**, 2823 (1998).

[17] R. Brun, R. Hagelberg, M. Hansroul, and J. C. Lassalle, version 3.15, Report No. CERN-DD-78-2-REV.

[18] S. Moch and P. Uwer, Nucl. Phys. B, Proc. Suppl. **183**, 75 (2008).

[19] D. Acosta *et al.*, Nucl. Instrum. Methods Phys. Res., Sect. A **494**, 57 (2002).

[20] K. Hagiwara, R. D. Peccei, D. Zeppenfeld, and K. Hikasa, Nucl. Phys. **B282**, 253 (1987).